Department of the Interior
U. S. Geological Survey [Reports-Openfile series]

345 Middlefield Road
Menlo Park, CA 94025

Continuous Tilt, Strain and Magnetic Field Measurements Near Four Earthquakes (M_L = 3.6 to 3.8) on the San Andreas Fault, California

TM
Cmc
Twomey

by

M. Malcolm J. S. Johnston, A. C. Jones, C. E. Mortensen and B. E. Smith*

yellow

Short Title: Tilt, Strain and Magnetic Measurements near Several Moderate Earthquakes

(*authors in alphabetical order)

Open-File Report 78-987

This report is preliminary and has not been edited or reviewed for conformity with Geological Survey standards and nomenclature.

INTRODUCTION

Four moderate earthquakes (M = 3.6 to 3.8) have occurred on the San Andreas fault in central California since October, 1977. These earthquakes are the first since 1974 to occur at this magnitude level within the array of tilt, strain, and magnetic instruments between Chalome (35.726N, 12,249 W) and San Francisco (37.79N, 122.23W) shown in Figure 1. They offer, therefore, one of the few opportunities to search for indications of precursive ground deformation. Furthermore, several other geophysical parameters such as resistivity, creek, radon, seismicity, geodetic strain, etc, are also monitored and allow comparisons for some of these events. This note reports comparative data and some possible implications in continuous strain, tilt, magnetic field and other measurements obtained from instruments within 10 km of the epicenters.

Figure 2a and Figure 2b are expanded maps of the epicentral regions near Parkfield, California (35.83N, 12.33W) and Bear Valley (36.57N, 121.19W) showing the earthquake locations, magnitudes and occurrence date and the locations of the various instruments. Further details of these earthquakes are listed in Table 1. Routine location of the epicenters places the Bear Valley earthquakes to the west of the San Andreas fault probably because of the velocity contrasts between the west and east side of the fault (Boore and Hill, 1973; Engdahl and Lee, 1976). Applying the results of Ellsworth (1978) and Engdahl and Lee (1976), these events locate on the fault, as shown. The shaded area indicates the location error. The earthquake location and depth errors are less than 0.5 and 0.9 km respectively. The source dimensions L are calculated assuming an average stress drop for many California earthquakes of 20 bars (Thatcher and Hanks, 1975) from the equation

$$M_L = 1.75 \log L + 3.75 \quad (1)$$

where M_L is the local magnitude. The source area A is given by L^2. The seismic moments M_o are calculated from the equation (Wyss and Brune, 1973)

$$M_o = 1.7\ M_L + 15.1 \quad (2)$$

The seismic slip S is estimated from the moment using the equation

$$S = M_o/\mu A \quad (3)$$

where the rigidity μ was taken to be 10^{11} dyne-cm.

EXPECTED CHANGES

Changes in geophysical parameters associated with earthquakes might be expected to occur both coincident with the event (coseismic) and preceding it (preseismic) by a time determined by the failure criteria within the fault zone. Coseismic tilt, strain and magnetic changes can be estimated for each of the events on the basis of dislocation models of the earthquake (Chinnery, 1963). The precedure appears justified since it provides quite accurate estimates of strains and displacements in the case of large earthquakes that rupture the earth's surface. The changes in stress from the dislocation solutions are used in the tectonomagnetic calculation (Johnston, 1978).

Estimates of likely coseismic tilt, strain and magnetic field changes at each of the monitoring sites in Figures 2a and 2b for each of the four earthquakes within 10 km or so of these sites are listed in Table 2. In each of the dislocation models used, the fault was assumed to be vertical right-lateral strike-slip. This assumption is well supported by the general focal mechanism solutions of events on the San Andreas. The geometry and focal parameters used were taken from Figures 2a and 2b and Table 1.

The question concerning changes that might be expected coseismically at each site is important in assessing whether signals should, or should not, have been seen. Because of the complex quadrapole nature of surface displacement fields expected around earthquakes, it is impossible on the basis of 'distance from the event' along to make this judgement. Locations exist near the epicenter for which the strain, for example, may be insignificant. Other locations, at greater distances, may experience detectable strains.

The possible sense of preseismic or precursory signals might be indicated by these models of the earthquake, since possible precursory behavior, such as preseismic slip should be related to the source mechanism of the earthquake. Current failure models provide no quantative estimates of either the amplitude or the duration of preseismic slip.

Based on the values in Table 2, if right-lateral preseismic-slip centered on the earthquake hypocenter occurred it would be most easily seen on the BVS instrument for the November 4 event. The strain and tilt for the December 15 event would be the next most easily detected. However, it is not all all clear whether the amount of aseismic slip, if it occurs at all, scales with the earthquake magnitude.

It is clear from the values of magnetic change listed in Table 2 that no coseismic changes in magnetic field should be observable with the measurement resolution of about 0.25 gammas evident in the magnetic difference field measurements (Smith and Johnston, 197). Again, however, if related changes in stress over a broader region and with a longer duration occurred, they would be most easily detected for the December 28, 1977, event on the magnetic difference record LG-GD.

DATA

The long-term records of north-south and east-west tilt at BVL, strain at BSI (N30 E), BVS2 (S30E), BVS3 (W), BV1S (S30 E) and magnetic differences LE-BV are plotted in Figure 3a. The earthquake occurrence times are shown with arrows. Daily rainfall is plotted with a bar proportional to the amount of rainfall at the nearest National Weather Service station (Pinnacles National Monument in the case of Bear Valley). Expanded plots for the five days before and after the occurrence time of the earthquakes are shown in Figure 3b for the November 4 event and Figure 3c for the December 15 event.

Similar long-term records of tilt at LGC, TUK and GOH and magnetic difference records BV-LG are plotted in Figure 4a. Daily rainfall at Parkfield is shown as bars and the earthquakes are shown as arrows. Expanded plots for the five days before and after the occurrence time of the earthquakes are shown in Figure 4b for the November 29 event and Figure 4C for the December 28 event.

DISCUSSION

For each of the events considered here, the available instrumentation was about six source dimensions or more from the hypocenter. For the November 29 and December 15 events the instruments were more than 10 source dimensions distance. Based on dislocation models, the event for which the tilt and strain instruments are most optimally located in order to detect coseismic and tilt is the one on November 4. If any preseismic slip occurred in or near the hypocentral area then it might be expected to be detected for this earthquake more than any of the others. The largest change would be in the sense of compression on the strain component BVS1. Compression would occur on BVS2, expansion on BVS3 and the tilt on BVY would be to the north. Figure 4 shows the amplitudes and directions of the calculated coseismic tilts and strains in relation to the earthquake epicenter and fault geometry. Varying the geometry and shape of slip patch centered on the hypocenter can effect the amplitudes of the strains seen on the various components. In general expected strain changes exceed tilt changes at this location.

Some changes in the BVS1 and BVS3 strain records in Figure 3a do appear to have occurred around the times of the November 4 event. The similar changes for the December 15 event apparently occurred after the earthquake (Figure 3c). Whereas, the dislocation models discussed previously would predict changes of opposite sense, the sense of change in strain is the same for these two components.

Some longer term accelerated strain compatable in sense with that expected for preseismic slip is seen most clearly on BVS3 stating about the beginning of October. The BVS2 record is incomplete at this time. Other than a change in sense on BVS1 at this time, the BVS1 record is sufficiently

complicated by unexplained short term changes of up to a micro-strain that visual identification of signal purpostely related to the earthquakes in November and December cannot be made unambiguously.

The time-expanded versions of the records for the November 4 event in Figure 3b do not show any indications of very short-term accelerated strain and tilts in the hours before the main shock. Some indication of relaxation type strain behavior are evident on BVS2 and BVS3. There is no good explanation at present for this behavior.

Increased magnetic changes occurred around the times of both the November 4 and the December 15 earhquakes in Bear Valley. These amounted to about 0.5 gammas above the yearly mean value. However, other changes of this amplitude occurred early in the year without any corresponding earthquakes of similar magnitude. Based on tectonomagnetic models of the San Andreas, the sense of change at this loction is compatable with an increase or concentration of stress in the Bear Valley region during early November and late December.

For the events at Parkfield on November 29 and December 28, the latter shoud have produced the biggest coseismic tilts on the tiltmeters GOH and TUK (Figure 2b). These tilts would be down to the NW direction for GOH and down to the NE at TUK. Unfortunately, around this time (mid December to late December) heavy rains fell in the area (Figure 4a) and may have also produced spurious tilts of meteorological origin. Tilt perturbations are evident in the records of TUK, LGC and perhaps GOH for the 15 days prior to the December 28 event. There is no way at present to determine any or all of these signals are earthquake related or rainfall related.

For more than an inch of rain in March earlier in the year no significant tilt change (Figure 4a) occurs on any of the instruments. The small

fluctuation on LGCN occurs before the rainfall starts. Distributed rainfall in May totaling more than an inch produced a possible slight positive tilt on GOHE and LGCE and a slight negative tilt on LGCN. However, other larger tilts occur at times of no rain. Because of possible non-linear effects of rainfall the changes in late December could still be, and probably are rainfall induced.

Considering the November 29 event, the tilts calculated from the dislocation models are generally all down to the SW with the largest occurring on LGC. There are no short term tilt perturbation evident in any the records for this event. Some long term accelerated tilting occurred at the beginning of October on GOH and LGC and perhaps also on TUK.

The expanded records for the two events in Figures 4b and 4c show no repeatable very short-term precursive behavior as pointed out for similar magnitude earthquakes considered by Johnston and Mortensen (1974). The observed coseismic steps do not agree in amplitude or direction with those calculated on the basis of dislocation models, as was found also in a larger study by McHugh and Johnston, 1976.

CONCLUSION

Although some interesting patterns are evident in the tilt, strain, and magnetic records obtained, particuarly at Bear Valley, during the four earthquakes considered here, there are no clear repeated signals that could be considered to be precursive in these data.

REFERENCES

Boore, D. M. and D. P. Hill, 1973, Wave Propagation Characteristice in Vicinity of the San Andreas Fault Proc. Conf. Tectonic Problems of the San Andreas Fault System. Ed. R. L. Kovach and A. Nur Stanford University Publications, P215-224.

Chinnery, M. A., 1963, The Stress Changes that Accompany Strike Slip Faulting Bull. Seismol. Soc. Amer., 53, 921-932.

Ellsworth, W., 1978, Private Communication.

Engdahl, E. R., and Lee, W. H. K., 1976, Relocation of Local Earthquakes by Seismic Ray Training J. Geophys. Res., 81, 4400-4406.

Johnston, M. J. S., 1978, Local Magnetic Field Variations and Stress Changes Near a Slip Discontinuity on the San Andreas fault, J. Geomag. Geoelec., (in press.).

Johnston, M. J. S., and C. E. Mortensen, 1979, Tilt precursors before earthquakes on the San Andreas fault, California, Science, 186, 1031-1034.

McHugh, S. & Johnston, M., 1976, Some short period nonseismic tilt perturbations and their relation to episodic slip on the San Andreas fault, J. Geophys. Res., 81, 6341-6346.

Smith, B. E., Johnston M. J., Burford, R. O. and Mueller, R. J. 1978, Magnetic Field Changes, Earthquakes and Creep events along the San Andreas Fault, 1974-1977. J. Geomag. Geoelec. (in press).

Thatcher, W. and T. C. Hanks, 1973, Source parameters of sourthern California earthquakes, J. Geophys. Res., 78, 8547-8576.

Wyss, M., and J. N. Brune, 1968, Seismic moment, stress, and source dimensions for earthquakes in the California-Nevada region, J. Geophys. Res., 73, 4681-4694.

FIGURE CAPTIONS

Figure 1. Map of central California showing tilt, strain and magnetometer installations.

Figure 2a. Expanded map of the Bear Valley area showing the instrument locations, earthquakes magnitudes, occurrence times epicenters (stars) and location error (shaded).

Figure 2b. Expanded map of the Parkfield area showing the earthquake epicenters, magnitudes and occurrence times and the instrument locations.

Figure 3a. Time-history plots for 1977 of tilt from the site. BVY, strain from sites, BV1S, BVS1, BVS2 and BVS3 and magnetic field diffeences between the sites BV, LE, QS, and LG. Note that BV1S is parallel to but 0.5 km from BVS2. The occurrence times of the earthquakes are shown with arrows and daily rainfall with bars proportional to the amount of rainfall.

Figure 3b. Expanded tilt, strain and magnetic difference time-history plots showing 10 days of data round the November 4, 1977 event.

Figure 3c. Expanded tilt, strain and magnetic difference time-history plots showing 10 days of data round the December 15, 1977 event.

Figure 4a. Time-history plots for 1977 of tilt from the sites LGC, GDH and TUK near Parkfield LGC, GDH, and AGC. The occurrence time of moderate earthquake ($M_L = 3.6$) are shown as arrows.

Figure 4b. Expanded tilt and magnetic difference time-history plots showing 10 days of data round the November 29, 1977 event.

Figure 4C. Expanded tilt and magnetic difference time-history plots showing 10 days of data round the December 28, 1977 event.

Figure 5. Coseismic strains and tilts expected at the Bear Valley sites on the basis of a dislocation 1.07 km in extend at the November 4, 1978, earthquake hypocenter. The size of the dislocation corresponds to the that shown in Table 1 and the amplitudes and azimuths of the tilts and strains are listed in Table 2. The scaling circles have radii of 1×10^{-2} μstrain or μradian and 2×10^{-2} μstrain or μradians respectively.

Table Captions

Table 1. Locations, occurrence times, magnitudes and depths of four moderate earthquakes that occurred in 1977 with instrumental arrays. Listed also are the source parameters (Length L, area A, moment M_o and slip S) calculated from the formulas in the text. For each earthquake the nearest instrument and its distance to the epicenter is identified.

Table 2. Tilts, strains, and magnetic changes calculated at the nearest instrument for each of the earthquakes in Table 1 on the basis of dislocation models at the earthquake hypocenter. The parameters used in the dislocation models are listed in Table 1 and the geometry is shown in Figures 2a and 2b.

TABLE 1

Time (GMT)	LAT.	LONG.	MAG.	Depth	Nearest Instrument	Dist. To Epicenter (km)	L (km)	A (Km^2)	M (Dyne-cm)	S (cm)
11-4-77 (1512)	$35^{o}34.2$	$121^{o}12.75$	3.6	5.8	BVY, BVS	1.7	1.82	0.67	1.6×10^{21}	2.3
11-29-77 (1642)	$35^{o}55.35$	$120^{o}29.9$	3.8	13	LGC	3.2	1.07	1.14	3.6×10^{21}	3.2
12-15-77 (1115)	$36^{o}34.6$	$121^{o}13.68$	3.7	10.2	BVY, BVS	2.6	0.94	0.97	2.4×10^{21}	2.5
12-28-77 (0259)	$36^{o}47.8$	$120^{o}23.4$	3.8	6	GDH	5.6	1.07	1.14	3.6×10^{21}	3.2

TABLE 2

Date of Earthquake	Magnitude	Strain Component	Calculated Coseismic Strain (μStrain)	Tiltmeter	Calculated Coseismic Tilt (μRad)	Tilt Azimuth	Magnetometer	Calculated Magnetic Change (Gammas)
11-4-77	3 . 6	BVS 1 (N30E)	$+53.1 \times 10^{-3}$	BVL	15.0×10^{-3}	177°	BV	0.0016
		BVS 2 (S30E)	$+28.0 \times 10^{-3}$					
		BVS 3 (W)	-24.0×10^{-3}					
11-29-77	3 . 8			LGC	1.5×10^{-3}	217°	LGC	0.003
				TUK	1.4×10^{-3}	219°		
				GDH	0.5×10^{-3}	207°		
12-15-77	3 . 7	BVS 1 (N30E)	11.7×10^{-4}	BVL	4.8×10^{-3}		BV	0.01
		BVX 2 (S30E)	$+ 6.23 \times 10^{-3}$					
		BVS 3 (W)	$- 4.46 \times 10^{-3}$					
12-28-77	3 . 8			GDH	3.4×10^{-3}	336°	GD	0.06
				TUK	3.9×10^{-3}	53°		
				LGC	0.9×10^{-3}	35°		

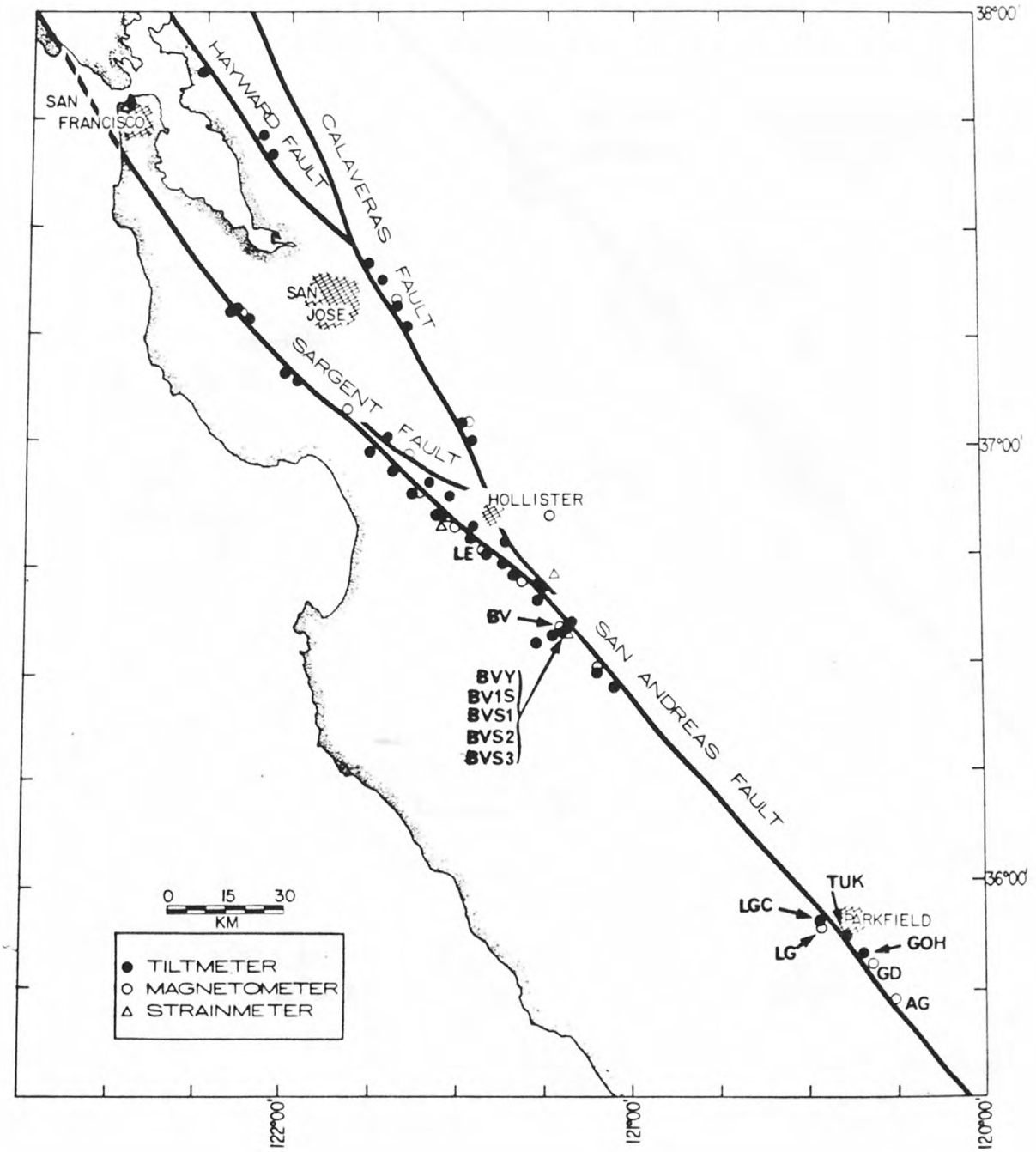
38°00'
37°00'
36°00'
122°00'
121°00'
120°00'
SAN FRANCISCO
HAYWARD FAULT
CALAVERAS FAULT
SAN JOSE
SARGENT FAULT
HOLLISTER
LE
BV
BVY
BV1S
BVS1
BVS2
BVS3
SAN ANDREAS FAULT
TUK
LGC
PARKFIELD
LG
GOH
GD
AG
0 15 30
KM
TILTMETER
MAGNETOMETER
STRAINMETER

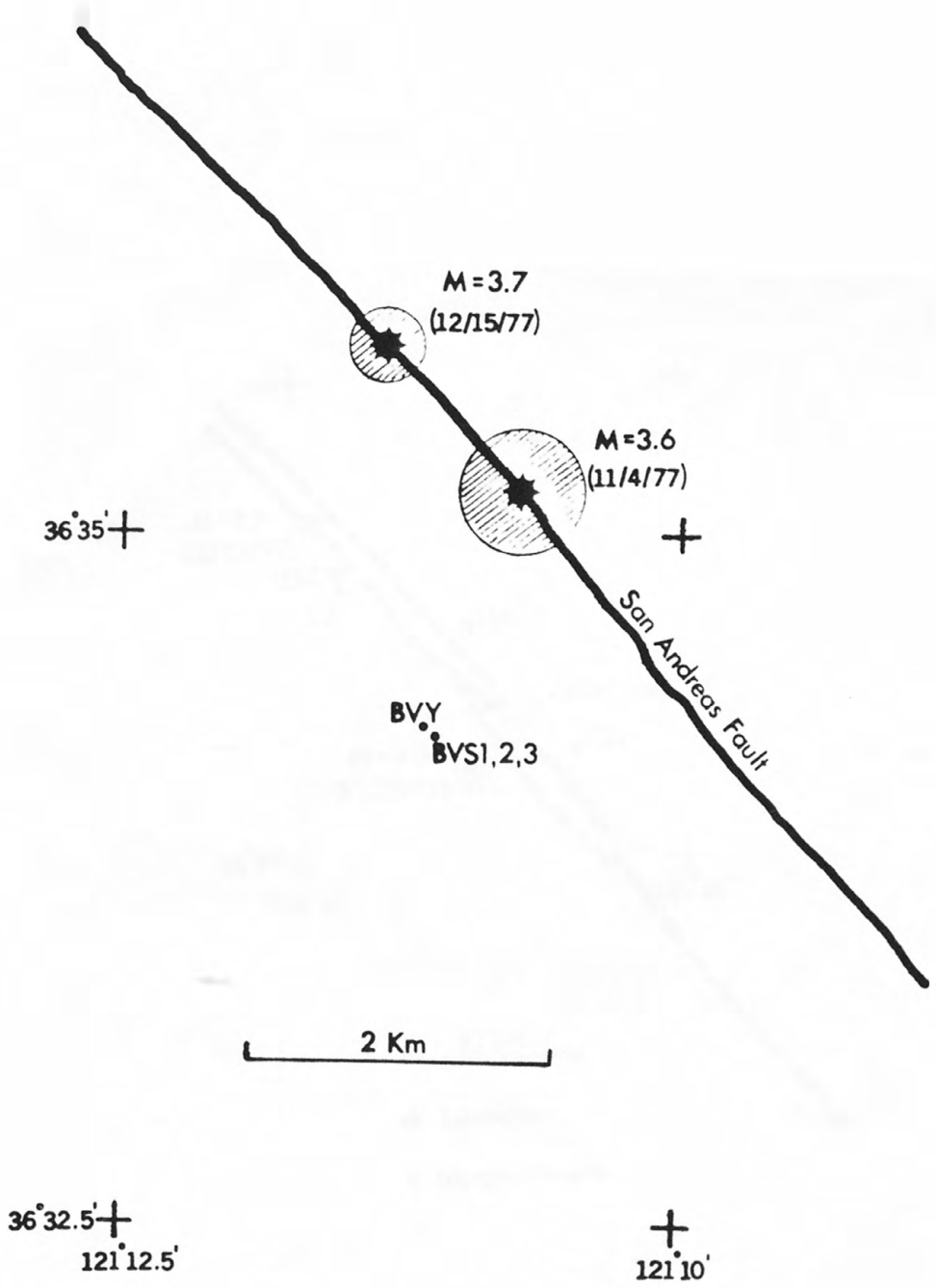
M = 3.7
(12/15/77)
M = 3.6
(11/4/77)
36°35'
San Andreas Fault
BVY
BVS1,2,3
2 Km
36°32.5'
121°12.5'
121°10'

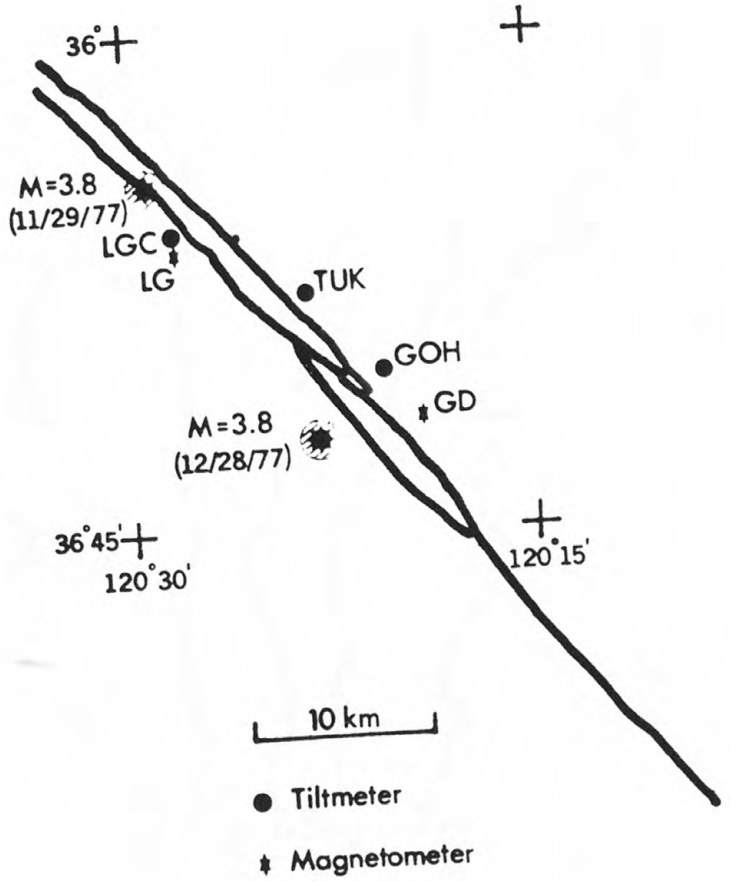
36°
M=3.8
(11/29/77)
LGC
LG
TUK
GOH
GD
M=3.8
(12/28/77)
36°45'
120°30'
120°15'
10 km
Tiltmeter
Magnetometer

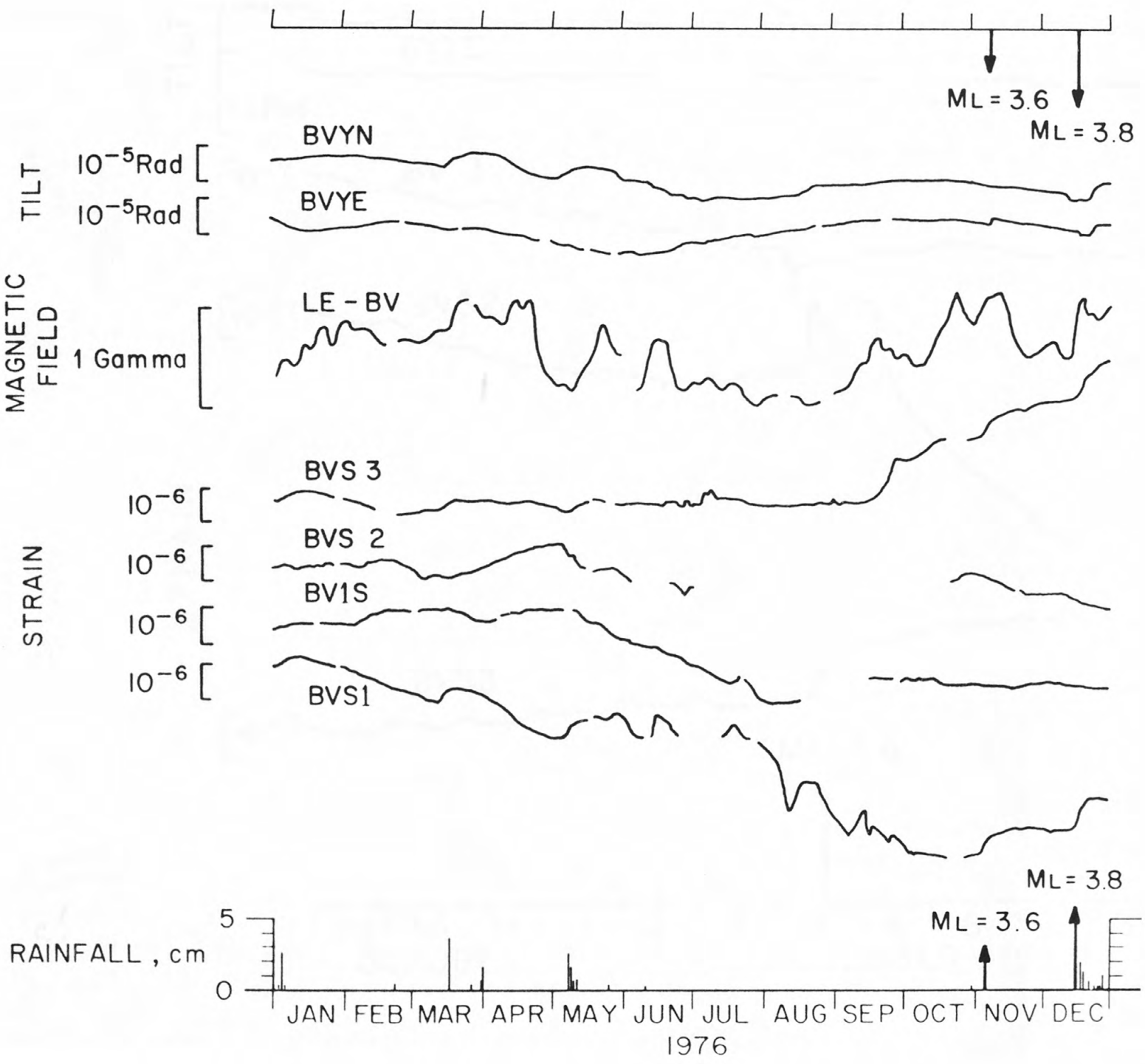
ML = 3.6
ML = 3.8
TILT
10⁻⁵Rad
BVYN
10⁻⁵Rad
BVYE
MAGNETIC FIELD
1 Gamma
LE - BV
STRAIN
10⁻⁶
BVS 3
10⁻⁶
BVS 2
10⁻⁶
BV1S
10⁻⁶
BVS1
ML = 3.8
ML = 3.6
RAINFALL , cm
5
0
JAN FEB MAR APR MAY JUN JUL AUG SEP OCT NOV DEC
1976

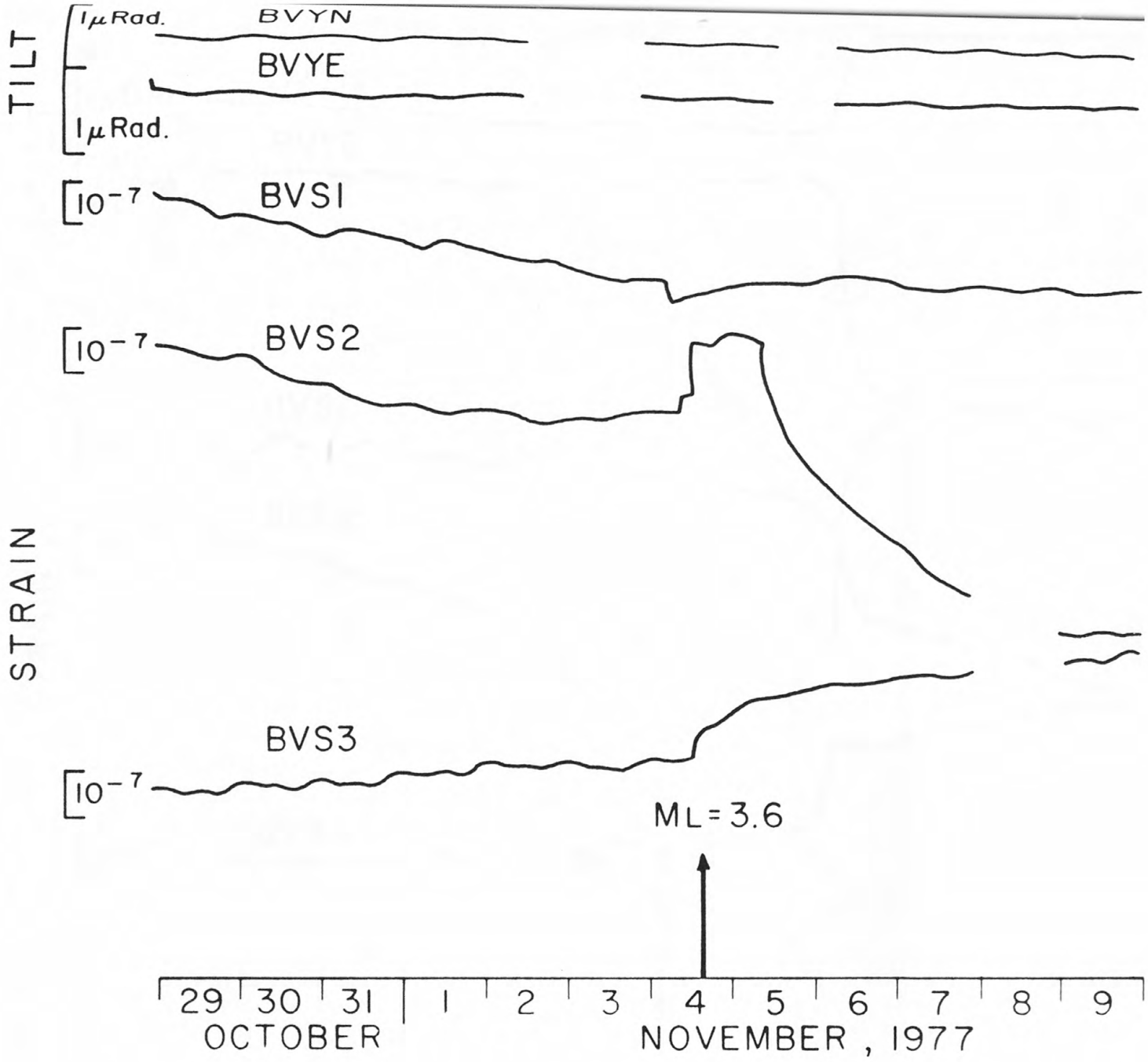
TILT
1μRad.
BVYN
BVYE
1μRad.
10⁻⁷
BVS1
10⁻⁷
BVS2
STRAIN
BVS3
10⁻⁷
ML=3.6
29
30
31
OCTOBER
1
2
3
4
5
6
7
8
9
NOVEMBER, 1977

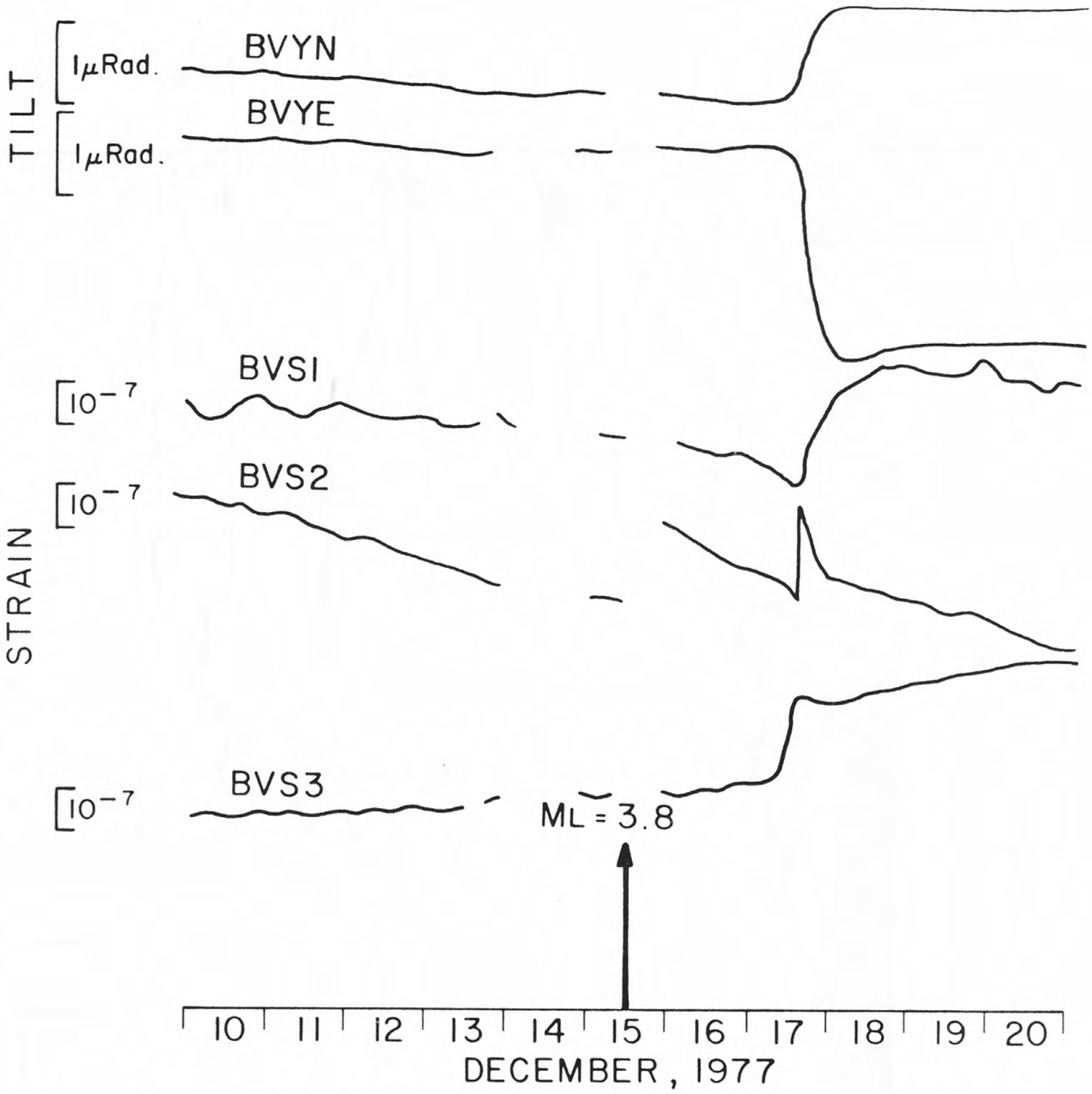
TILT
1μRad.
BVYN
1μRad.
BVYE
STRAIN
10⁻⁷
BVS1
10⁻⁷
BVS2
10⁻⁷
BVS3
ML = 3.8
10
11
12
13
14
15
16
17
18
19
20
DECEMBER, 1977

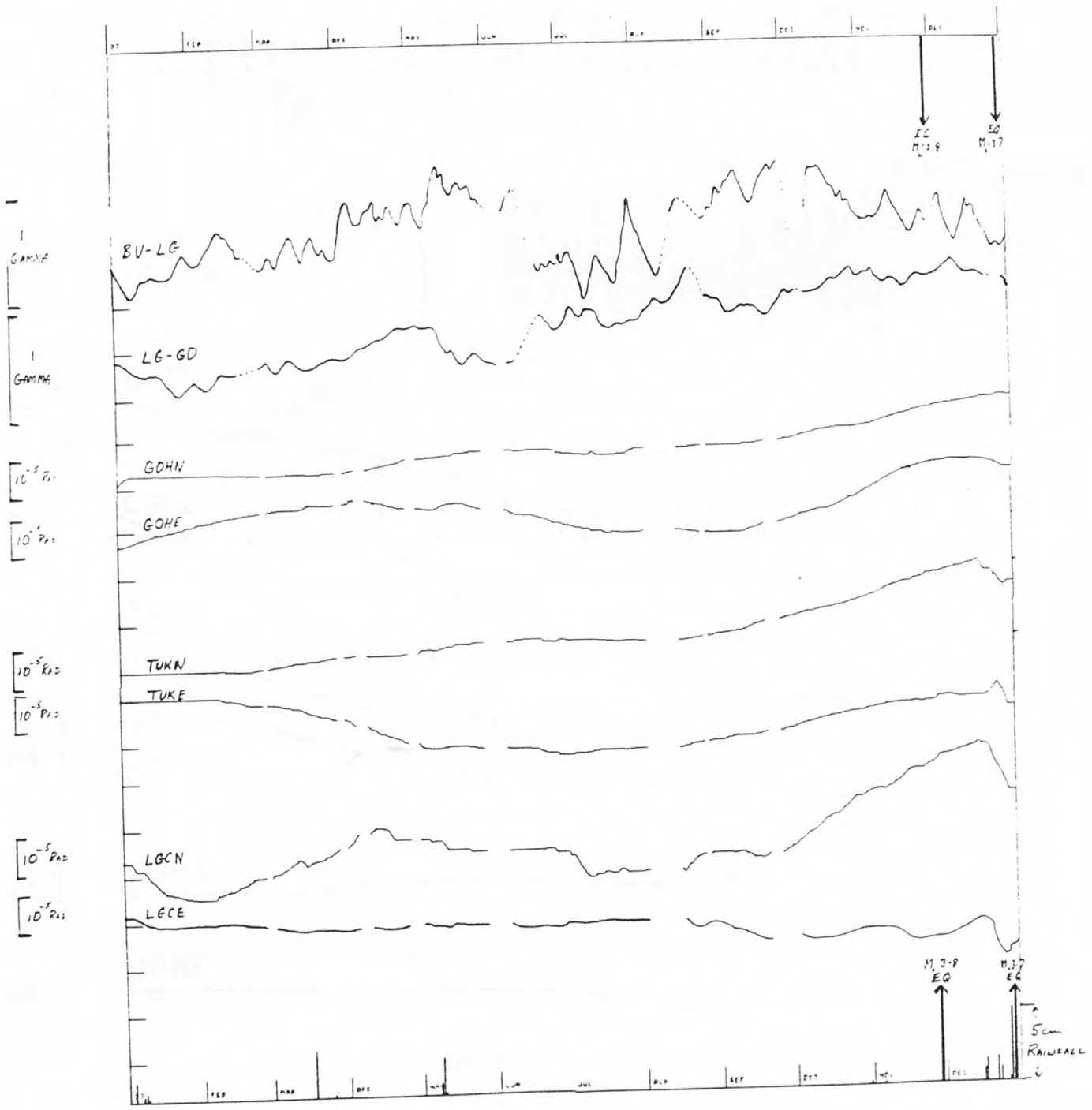
EQ M 3.8
EQ M 3.7
1 GAMMA
BV-LG
1 GAMMA
LG-GD
GDHN
GDHE
TUKN
TUKE
LGCN
LGCE
M 3.8 EQ
M 3.7 EQ
5cm RAINFALL

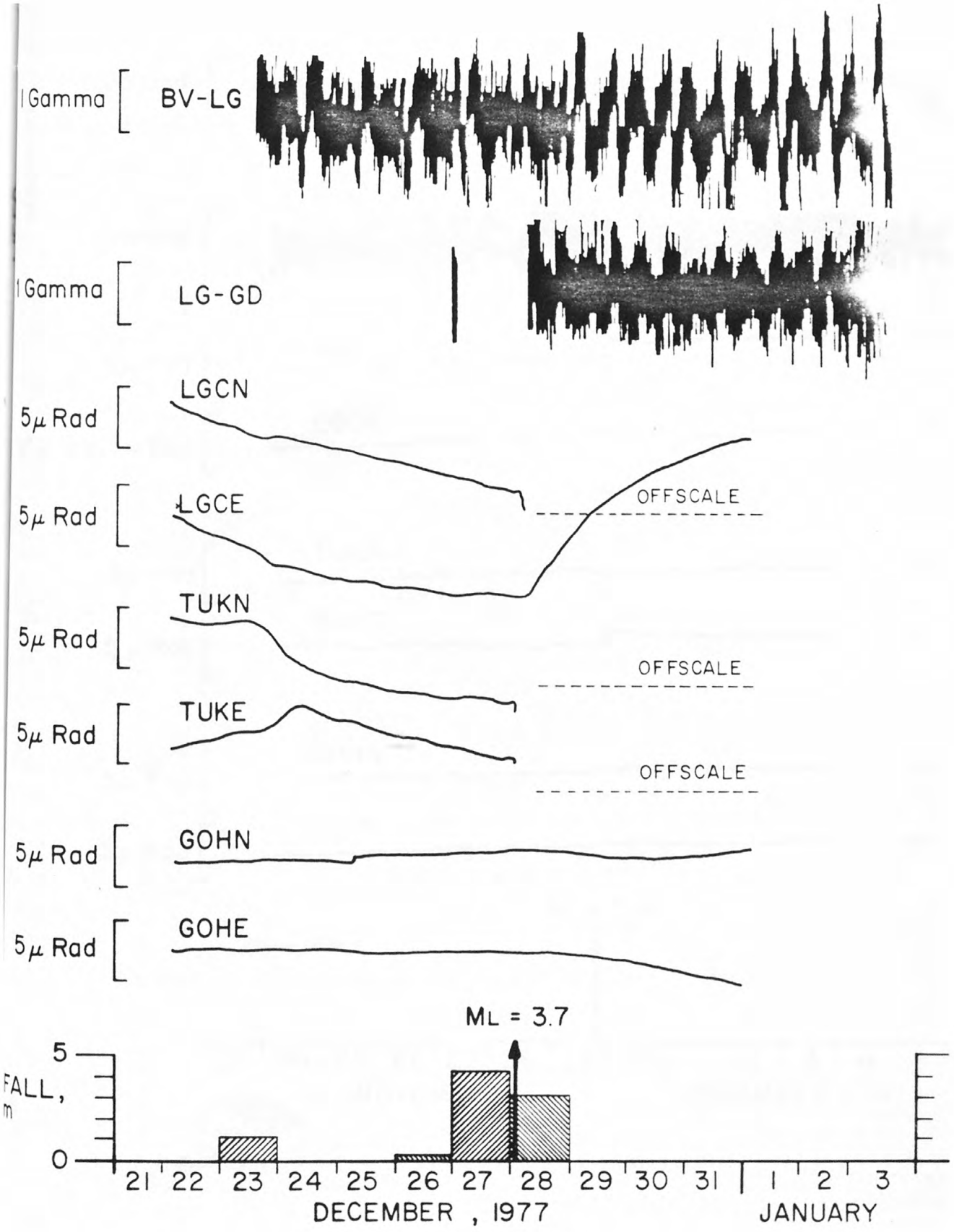
1 Gamma
BV-LG
1 Gamma
LG-GD
5μ Rad
LGCN
5μ Rad
LGCE
OFFSCALE
5μ Rad
TUKN
OFFSCALE
5μ Rad
TUKE
OFFSCALE
5μ Rad
GOHN
5μ Rad
GOHE
ML = 3.7
5
FALL,
m
0
21 22 23 24 25 26 27 28 29 30 31 1 2 3
DECEMBER , 1977
JANUARY

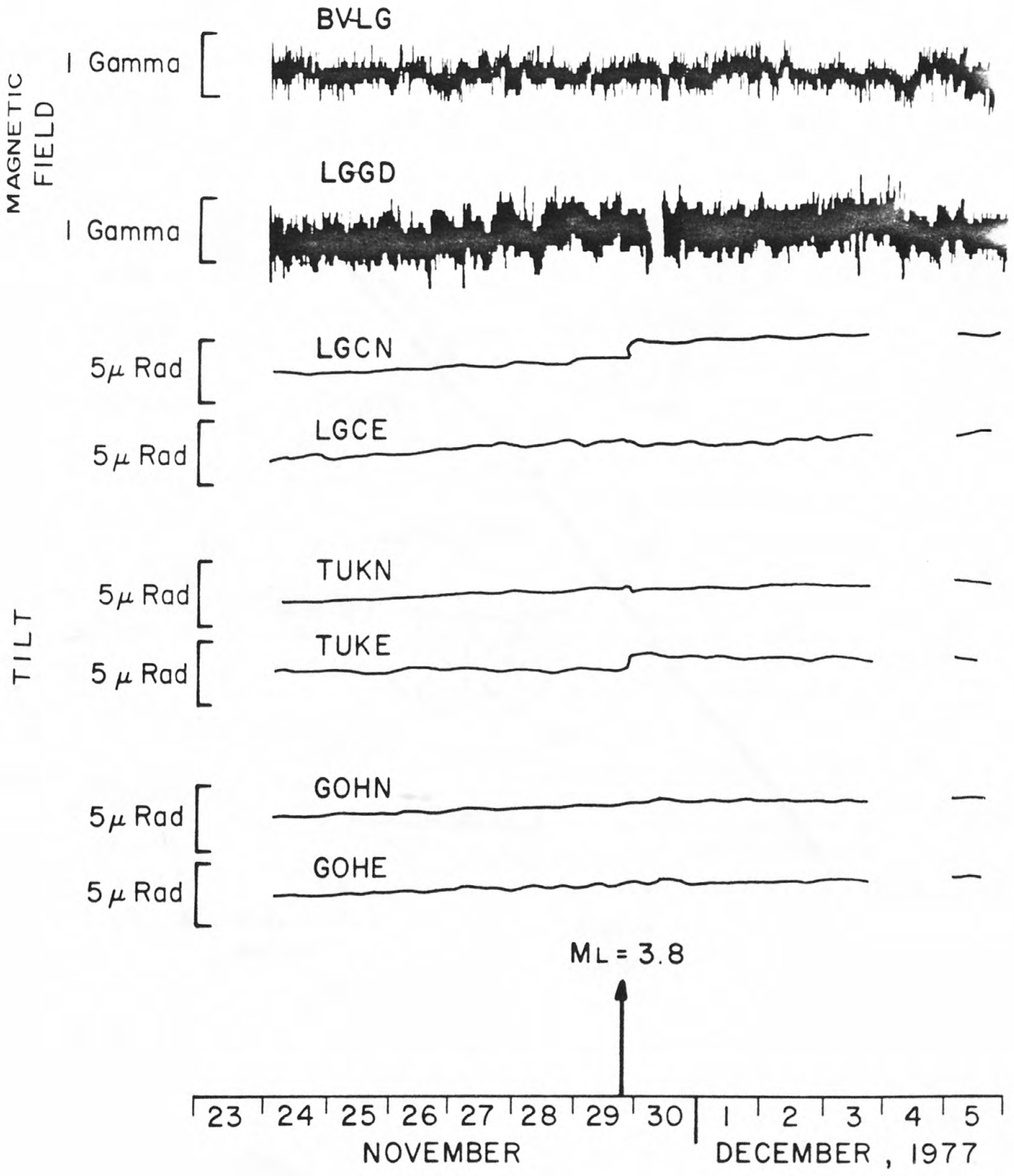
MAGNETIC FIELD
BV-LG
1 Gamma
LGGD
1 Gamma
LGCN
5μ Rad
LGCE
5μ Rad
TILT
TUKN
5μ Rad
TUKE
5 μ Rad
GOHN
5μ Rad
GOHE
5μ Rad
ML = 3.8
23 24 25 26 27 28 29 30 1 2 3 4 5
NOVEMBER
DECEMBER , 1977

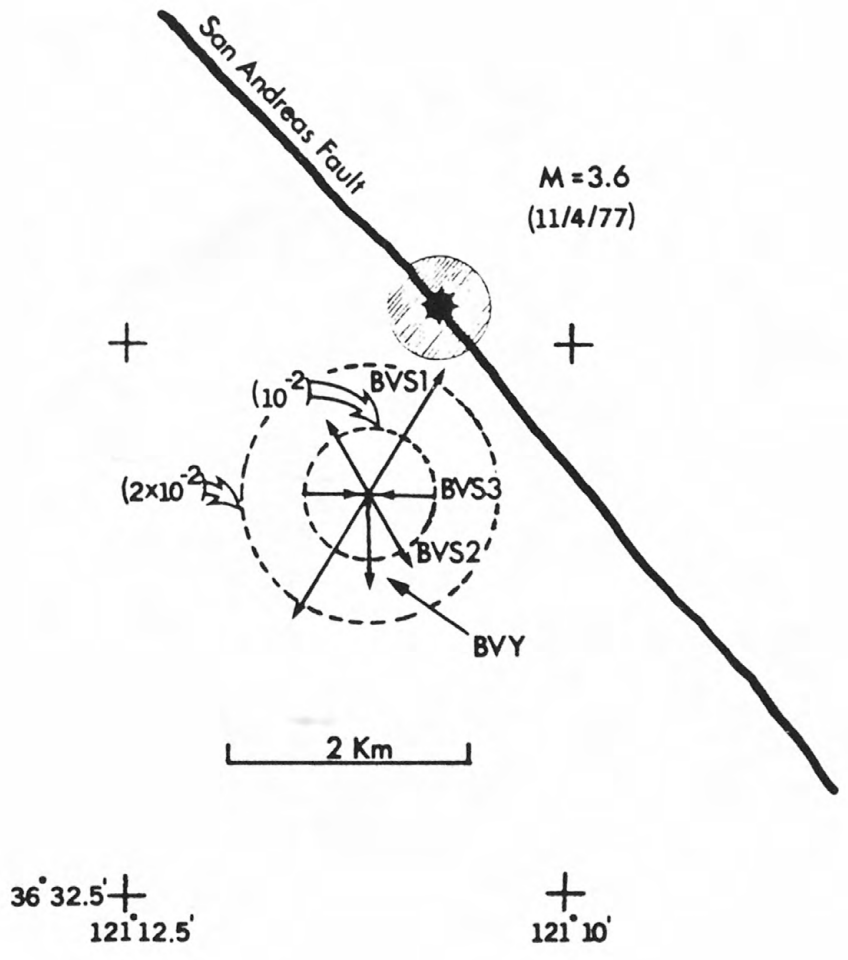
San Andreas Fault
M=3.6
(11/4/77)
(10^-2
BVS1
(2x10^-2
BVS3
BVS2
BVY
2 Km
36°32.5'
121°12.5'
121°10'